Bulletin of PFUR Series *Mathematics. Information Sciences. Physics.* No 3 (2). 2010. Pp. 136–142

Физика

UDC 517.958: 53, 519.62/.642

Time–Periodic Solitons in the Damped–Driven Nonlinear Schrödinger Equation

E. V. Zemlyanaya[*], N. V. Alexeeva[†], T. C. van Heerden[†]

[*] *Laboratory of Information Technologies*
Joint Institute for Nuclear Research
Joliot-Curie 6, 141980 Dubna, Moscow region, Russia
[†] *Department of Mathematics*
University of Cape Town, Rondebosch 7701, South Africa

We study localised attractors of the parametrically driven damped nonlinear Schrödinger equation. Time-periodic solitons of this equation are obtained as solutions of the boundary-value problem on a two-dimensional domain. We classify stability and bifurcations of periodic solitons and their complexes.

Key words and phrases: nonlinear Schrödinger equation, temporally periodic solitons, newtonian iterative scheme, stability, bifurcations.

1. Introduction

This paper deals with the parametrically driven damped nonlinear Schrödinger equation,

$$i\psi_t + \psi_{xx} + 2|\psi|^2\psi - \psi = h\psi^* - i\gamma\psi. \tag{1}$$

Here $\gamma > 0$ is the damping coefficient, and $h > 0$ the amplitude of the parametric driver. Equation (1) describes the nonlinear Faraday resonance in a vertically oscillating water trough [1, 2] and the effect of phase-sensitive amplifiers on solitons in optical fibers [3,4]. The same equation controls the magnetization waves in an easy-plane ferromagnet placed in a combination of a static and microwave field [5] and the amplitude of synchronized oscillations in vertically vibrated pendula lattices [6, 7].

Localised stationary or periodic solutions of Eq. (1) exist only if $h > \gamma$. When $h > h_c$, where

$$h_c = \sqrt{1+\gamma^2}, \tag{2}$$

any localised solution is unstable to spatially-extended perturbations. The evolution of this instability leads to the spatiotemporal chaos. Two stationary soliton solutions of Eq. (1) are well known [5]:

$$\psi_\pm(x) = A_\pm e^{-i\vartheta_\pm}\mathrm{sech}(A_\pm x), \tag{3}$$

where

$$A_\pm = \sqrt{1 \pm \sqrt{h^2-\gamma^2}}, \quad \vartheta_+ = \frac{1}{2}\arcsin\frac{\gamma}{h}, \quad \vartheta_- = \frac{\pi}{2} - \vartheta_+.$$

The soliton $\psi_-(x)$ exists for $\gamma \leqslant h \leqslant \sqrt{1+\gamma^2}$ and is unstable for all h and γ. The soliton $\psi_+(x)$ exists for all $h \geqslant \gamma$; its stability properties depend on γ and h.

When $\gamma > 0.356$, the ψ_+ soliton is stable for all h in the range $\gamma < h < h_c(\gamma)$. When $\gamma < 0.356$, on the other hand, the soliton (3) is only stable for $\gamma < h < h_{\mathrm{Hopf}}(\gamma)$, where the value $h_{\mathrm{Hopf}}(\gamma)$ lies between γ and $h_c(\gamma)$ (dashed curve in Fig. 1). As we increase h past $h_{\mathrm{Hopf}}(\gamma)$ keeping $\gamma < 0.356$ fixed, the stationary soliton loses its stability to a time-periodic soliton [5, 8]. The transformation scenario arising as h is increased

Received 28th November, 2009.
EVZ was supported by the DST grant under the JINR/RSA Research Collaboration Programme and partially supported by RFBR (grant No.09-01-00770).

further, depends on the value of γ. According to the numerical simulations of [9], for γ smaller than approximately 0.26 the periodic soliton follows a period-doubling route to temporal chaos. In a wide region of h values above the chaotic domain, the equation does not support any stable spatially-localised solutions. In this "desert" region, the only attractor determined in direct numerical simulations was the trivial one, $\psi = 0$. Finally, for even larger values of h, the unstable soliton seeds the spatio-temporal chaos [9].

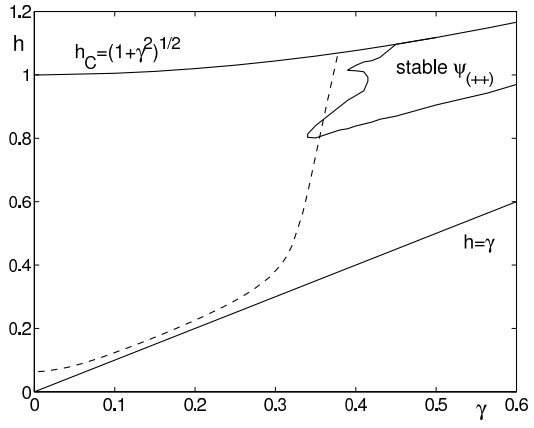

Figure 1. **The existence and stability chart of the stationary two-soliton complexes. For each γ, the region of existence of the complexes extends in the direction of larger h, beyond the value h_c**

As h is increased for the fixed γ larger than 0.275 (but smaller than 0.365), the soliton follows a different transformation scenario. Here, the period-doubling cascade does not arise and the soliton death does not occur. The periodic soliton remains stable until it yields directly to a spatio-temporal chaotic state [9].

In a short intermediate range of γ-values, $0.26 < \gamma < 0.275$, we have a combination of the above two scenarios. The increase of h for the fixed γ results in the period-doubling of the soliton, followed by the temporal-chaotic and "desert" regions. However, as we continue to raise h, an inverse sequence of bifurcations is observed which brings the stable single-periodic soliton back. On further increase of h, it loses its stability to a spatio-temporal chaotic state [9].

In the region $\gamma > 0.356$, where the stationary one-soliton solution ψ_+ soliton is stable for all h in the range $\gamma < h < h_c(\gamma)$ [5], no periodic solutions can detach from this stationary branch. However, the stationary *two*-soliton solutions do undergo Hopf bifurcations here [10]. The stability domain for the two-soliton complex ($\psi_{(++)}$) on the (γ, h)-plane is shown in Fig. 1. It is bounded by the curve $h_c(\gamma)$ on the top. Another solid curve demarcates the Hopf bifurcation points of stationary two-soliton solutions [11].

The purpose of our work is to follow the transformations of temporally periodic solutions of Eq. (1) as its parameters are varied, identify the arising bifurcations and eventually explain the attractor chart for this equation which was compiled using direct numerical simulations in Ref. [9]. We will also add missing details to this chart such as coexisting attractors in cases of bistability.

2. Periodic Solitons as Solutions of a 2D Boundary-Value Problem

So far, the direct numerical simulation has been the only way to obtain periodic solutions and study their stability. The shortcoming of this method is that simulations capture only *stable* solutions. This means that the actual mechanisms and details

of the transformations (which are bifurcations involving both stable and unstable solutions) remain unaccessible. Neither can simulations be used to identify alternative attractors in cases of bi- or multi-stability.

We propose a new approach to the analysis of these hidden mechanisms. Instead of solving Eq. (1) with some initial condition and determining the resulting attractor by running the computation for a sufficiently long time, we will be looking for periodic solutions by solving Eq. (1) as a boundary-value problem on a two-dimensional domain $(-\infty,\infty)\times(0,T)$. The boundary conditions will be set as

$$\psi(x,t)=0 \quad \text{as } x\to\pm\infty, \quad \text{and} \quad \psi(x,t+T)=\psi(x,t). \tag{4}$$

The period T is regarded as an unknown, along with the solution $\psi(x,t)$. Letting $\tilde{t}=t/T$ $(0<\tilde{t}<1)$ and defining $\tilde{\psi}(x,\tilde{t})=\psi(x,t)$, the boundary-value problem (1), (4) can be reformulated on a strip $(-L,L)\times(0,1)$ (where L is chosen to be sufficiently large):

$$i\tilde{\psi}_{\tilde{t}}(x,\tilde{t})+T\Phi(\tilde{\psi}(x,\tilde{t}),h,\gamma)=0, \quad \tilde{\psi}(\pm L,\tilde{t})=0, \quad \tilde{\psi}(x,0)=\tilde{\psi}(x,1). \tag{5}$$

Here,

$$\Phi(\tilde{\psi}(x,\tilde{t}),h,\gamma)=\tilde{\psi}_{xx}+2|\tilde{\psi}|^2\tilde{\psi}-\tilde{\psi}-h\tilde{\psi}^*+i\gamma\tilde{\psi}.$$

The periodic solutions are path-followed in h for the fixed γ, with the Hopf bifurcation points of the static solution used as starting points in the continuation process (see Fig. 1). We employ a predictor-corrector algorithm [12] with a fourth-order Newtonian iteration at each h. Most calculations were performed on the domain $(-L,L)=(-50,50)\times(0,1)$, with the stepsizes of the finite-difference approximation being $\Delta x=0.05$ and $\Delta\tilde{t}=0.01$.

For the graphical representation of solutions, we use the average energy, defined by

$$\overline{E}=\frac{1}{T}\int\limits_0^T E\mathrm{d}t, \quad E=\int\limits_{-\infty}^{\infty}\left[|\psi_x|^2+|\psi|^2-|\psi|^4+h\frac{\psi^2+\psi^{*2}}{2}\right]\mathrm{d}x. \tag{6}$$

Stability of solutions is classified by examining the Floquet multipliers of the corresponding linearised equation. Details are in [11].

3. Results of Numerical Study

In [11, 13], we applied the above numerical approach to periodic solitons with $\gamma=0.3$, 0.265, and 0.565 as representative sections of various parts of the attractor chart. Here, we focus on the case $\gamma=0.35$ for which the periodic one- and two-soliton solutons coexist (see Fig. 1).

We start with the one-soliton solutions. Our numerical continuation shows that in the case $\gamma=0.35$, the transformation of the solution is similar to the one in the case $\gamma=0.3$; see Fig. 2. The left-end point of each of the two curves in that figure corresponds to the stationary single-soliton solution ψ_+. The corresponding value of h equals $h=0.385$ for $\gamma=0.30$ and $h=0.7500$ for $\gamma=0.35$. At this value of h the stationary ψ_+ soliton undergoes the Hopf bifurcation and a stable *periodic* soliton is born. At the turning point $h_{\rm sn}$, the periodic solution loses its stability. Numerically, the turning-point value is $h_{\rm sn}=0.8761$ for $\gamma=0.30$ and $h_{\rm sn}=1.0186$ for $\gamma=0.35$. The end point of the unstable branch ($h=0.61$ for $\gamma=0.30$ and $h=0.760$ for $\gamma=0.35$) corresponds to a stationary three-soliton complex $\psi_{(-+-)}$.

Solutions at representative points are shown in Fig. 3. Near the leftmost point of the ($\gamma=0.3$)-curve in Fig. 2, the periodic solution looks like a single soliton with a periodically oscillating amplitude and width (Fig. 3(a)). As we continue along the curve, the oscillating solution evolves into a three-hump structure which may be interpreted as a triplet of solitons. Near the end point of the curve, the amplitude of

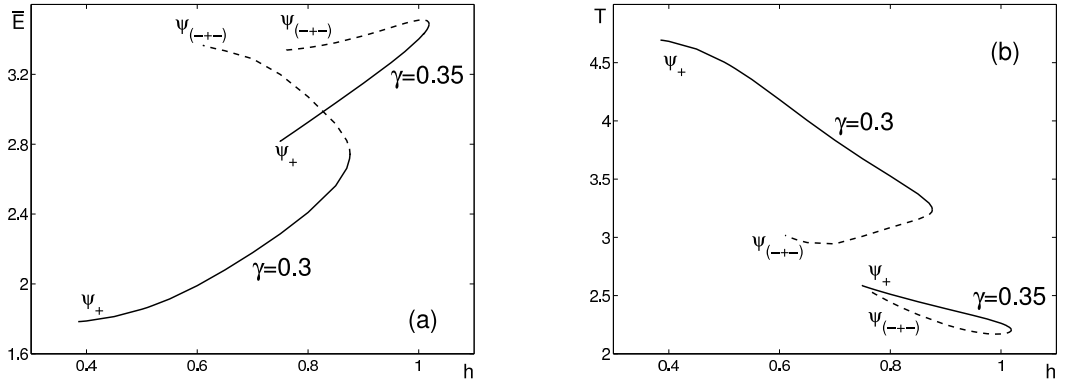

Figure 2. **The average energy (a) and the period (b) of the periodic solutions with** $\gamma = 0.30$ **and** $\gamma = 0.35$**. The solid curves show the stable and the dashed one unstable branches**

oscillations decreases (Fig. 3(b)) and we arrive at the stationary three-soliton complex.

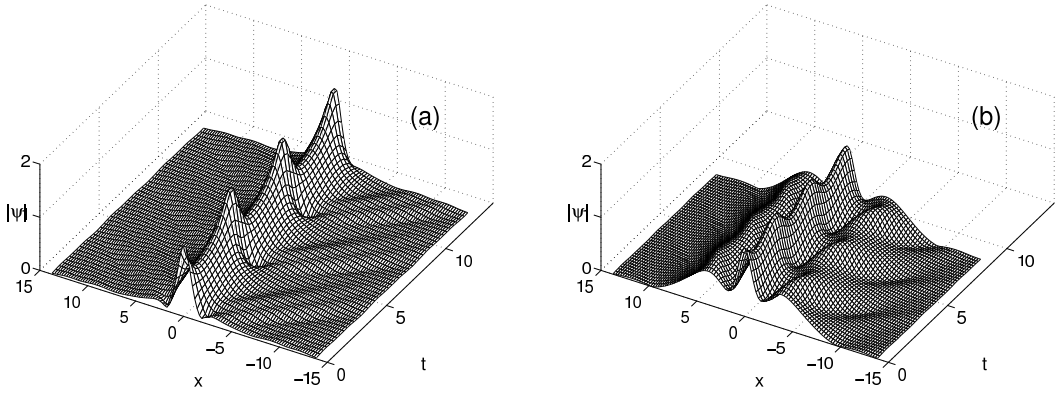

Figure 3. **The absolute value of the periodic solution with** $\gamma = 0.3$**: (a)** $h = 0.55$**,** $T = 4.356$**; (b)** $h = 0.64$**,** $T = 2.967$**. In each case several periods of oscillation are shown**

We now turn to the two-soliton complexes. For γ in the range $0.34 < \gamma < 0.40$ the stability domain of the stationary two-soliton complex is bounded by *two* Hopf bifurcations (see Fig. 1). Each Hopf bifurcation gives rise to a temporally periodic two-soliton solution. Let, for instance, $\gamma = 0.35$. Here, the "lower" Hopf bifurcation occurs at $h_{H1} = 0.806$. This bifurcation is supercritical; for $h < h_{H1}$, the unstable stationary two-soliton solution is replaced by a stable periodic two-soliton complex. As we continue the periodic complex in the direction of smaller h, at some point ($h = 0.79$) it loses its stability to a double-periodic complex of two solitons. As we continue the unstable branch, it makes a number of turns (Fig. 4), the spatiotemporal complexity of the solution increases (Fig. 5) but it never regains its stability. The "upper" Hopf bifurcation occurs at $h_{H2} = 0.832$. This bifurcation is subcritical: the emerging periodic branch is unstable and coexists with the stable stationary branch (i.e. the periodic branch continues in the direction of *lower* h, see Fig. 6). The entire branch is unstable in the case $\gamma = 0.35$. However, the increase of γ results in the stabilization of the periodic two-soliton solution. This is exemplified by $\gamma = 0.38$ — see the second branch in Fig. 6 which features a stable interval $h_1 < h < h_2$, with $h_1 = 0.9415$ and $h_2 = 1.015$. At the bifurcation points $h_{1,2}$ the periodic two-soliton solution loses stability to a quasi-periodic two-soliton complex.

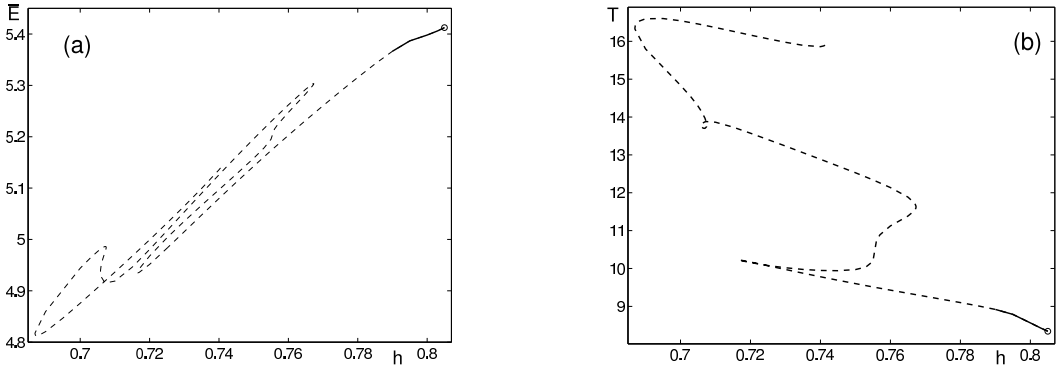

Figure 4. **The first branch of the two-soliton periodic solution for $\gamma = 0.35$. (a): the average energy; (b): the period of the solution. The solid curve shows the stable and the dashed one unstable branch**

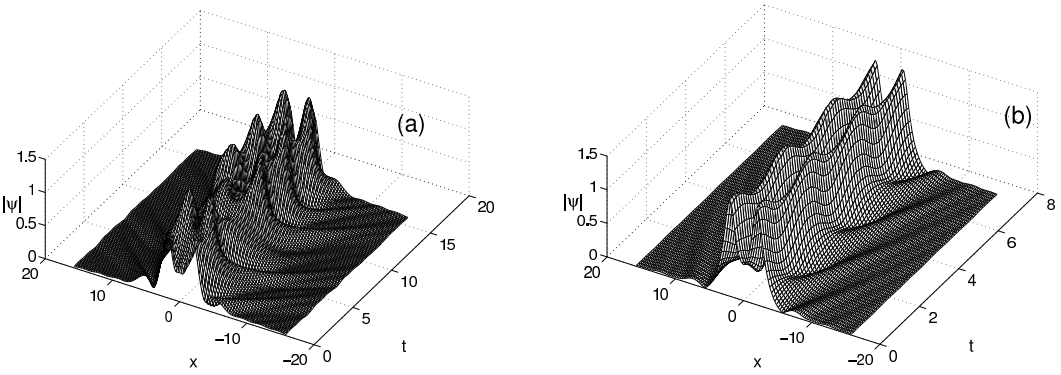

Figure 5. **(a) A two-soliton periodic solution with complex temporal behaviour arising at the end point of the curve presented in Fig. 4. Here $h = 0.741$, $T = 15.9$; figure shows the solution over one period. (b) The two-soliton periodic solution on the stable branch shown in Fig. 6. Several periods of oscillation are shown. Here $\gamma = 0.38$, $h = 0.95$, $T = 2.476$**

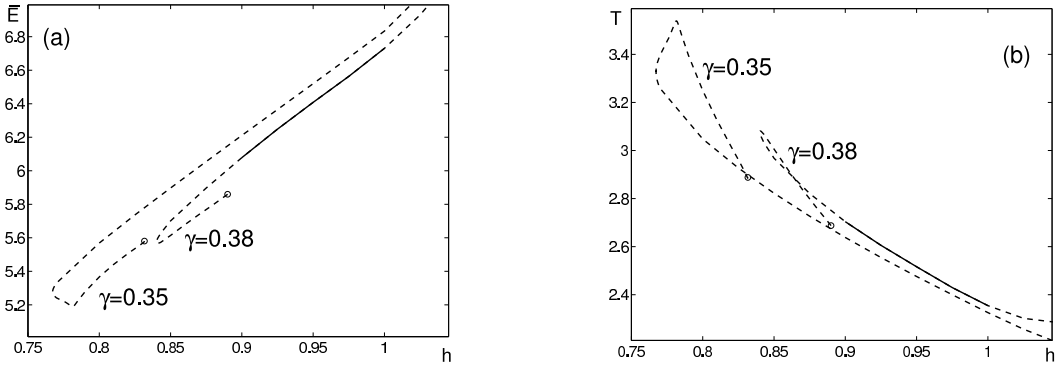

Figure 6. **The second branch of the periodic two-soliton solution with $\gamma = 0.35$ and $\gamma = 0.38$. The solid curve marks the stable and the dashed one unstable branch. The circles indicate the starting point of the continuation (the point where the stationary two-soliton complex undergoes the Hopf bifurcation)**

4. Conclusions

Our numerical approach allows to answer a number of questions raised by the one-soliton attractor chart of Ref. [9]. One such question is of the existence of periodic solutions with higher periods for γ in the interval $0.275 < \gamma < 0.365$. According to Fig. 2, the periodic one-soliton solution with γ in that region does not undergo any period-doubling bifurcations; hence there cannot be any 2T, 4T etc solutions here, neither stable nor unstable.

The absence of higher-periodic solutions should not be considered as a signature of "reduced soliton complexity" though. We have discovered a number of stable periodic two-soliton complexes in the region of large damping coefficients. These do undergo period-doubling bifurcations, as a result of which there is wealth of stable higher-periodic multisoliton solutions. The complete classification of the periodic solitons and their complexes will be addressed in future publications.

References

1. *Elphick C., Meron E.* Localized Structures in Surface Waves // Phys. Rev. A. — 1989. — Vol. 40. — Pp. 3226–3229.
2. *Chen X. N., Wei R. J.* Dynamic Behaviour of a Nonpropagating Soliton Under a Periodically Modulated Oscillation // J. Fluid Mech. — 1994. — Vol. 259. — Pp. 291–303.
3. *Longhi S.* Ultrashort-Pulse Generation in Degenerate Optical Parametric Oscillators // Opt. Lett. — 1995. — Vol. 20. — P. 695–697.
4. *Sánchez-Morcillo V. J. et al.* Vectorial Kerr-cavity solitons // Opt. Lett. — 2000. — Vol. 25. — Pp. 957–959.
5. *Barashenkov I. V., Bogdan M. M., Korobov V. I.* Stability Diagram of the Phase-Locked Solitons in the Parametrically Driven, Damped NLS equation // Europhys. Lett. — 1991. — Vol. 15. — Pp. 11–118.
6. *Denardo B. et al.* Observations of Localized Structures in Nonlinear Lattices – Domain Walls and Kinks // Phys. Rev. Lett. — 1992. — Vol. 68. — Pp. 730–1733.
7. *Alexeeva N. V., Barashenkov I. V., Tsironis G. P.* Impurity-Induced Stabilisation of Solitons in Arrays of Parametrically Driven Nonlinear Oscillators // Phys. Rev. Lett. — 2000. — Vol. 84. — Pp. 3053–3056.
8. *Alexeeva N. V., Barashenkov I. V., Pelinovsky D. E.* Dynamics of the Parametrically Driven NLS Solitons Beyond the Onset of the Oscillatory Instability // Nonlinearity. — 1999. — Vol. 12. — Pp. 103–140.
9. *Bondila M., Barashenkov I. V., Bogdan M. M.* Topography of Attractors of the Parametrically Driven Damped NLS Equation // Physica D. — 1995. — Vol. 87. — Pp. 314–320.
10. *Barashenkov I. V., Zemlyanaya E. V.* Stable Complexes of Parametrically Driven, Damped NLS Solitons // Phys. Rev. Lett. — 1999. — Vol. 83. — Pp. 2568–2571.
11. *Zemlyanaya E. V., Barashenkov I. V., Alexeeva N. V.* Temporally-Periodic Solitons of Parametrically Driven Damped NLS // Lecture Notes in Computer Sciences. — 2009. — Vol. 5434. — Pp. 139–150.
12. *Zemlyanaya E. V., Barashenkov I. V.* Numerical Study of Multisoliton Complexes in Parametrically Driven, Damped NLS Equation // Math. Modelling. — 2004. — Vol. 16, issue 11. — Pp. 3–14.
13. *Zemlyanaya E. V., Alexeeva N. V.* Oscillating Solitons of the Damped-Driven NLS Equation // Theor. and Math. Physics. — 2009. — Vol. 159. — Pp. 536–544.

УДК 517.958: 53, 519.62/.642

Периодические по времени солитоны в нелинейном уравнении Шрёдингера с диссипацией и накачкой

Е. В. Земляная[*], **Н. В. Алексеева**[†], **Т. С. ван Херден**[†]
[*] *Лаборатория информационных технологий*
Объединённый институт ядерных исследований
ул. Жолио-Кюри, д.6, Дубна, Московская область, 141980, Россия
[†] *Факультет математики*
Кейптаунский Университет, Рондебош 7701, Южная Африка

Изучаются локализованные аттракторы нелинейного уравнения Шрёдингера с диссипацией и параметрической накачкой. Периодические по времени солитоны этого уравнения получены как решение граничной задачи в двумерной области. Исследуются устойчивость и бифуркации периодических солитонов и их комплексов.

Ключевые слова: нелинейное уравнение Шрёдингера, периодические солитоны, ньютоновские итерационные схемы, устойчивость, бифуркации.